Bioanalysis

DOI: 10.1002/ange.201308972

Real-Time Monitoring of Auxin Vesicular Exocytotic Efflux from Single Plant Protoplasts by Amperometry at Microelectrodes Decorated with Nanowires**

Jun-Tao Liu, Liang-Sheng Hu, Yan-Ling Liu, Rong-Sheng Chen, Zhi Cheng, Shi-Jing Chen, Christian Amatore, Wei-Hua Huang, and Kai-Fu Huo**

Abstract: *Recent biochemical results suggest that auxin (IAA) efflux is mediated by a vesicular cycling mechanism, but no direct detection of vesicular IAA release from single plant cells in real-time has been possible up to now. A TiC@C/Pt-QANFA micro-electrochemical sensor has been developed with high sensitivity in detection of IAA, and it allows real-time monitoring and quantification of the quantal release of auxin from single plant protoplast by exocytosis.*

The transport and release of specific biochemical or chemical messengers by vesicular exocytosis are essential in many biological processes.[1] Vesicular exocytosis is organized by precise molecular machineries that mediate vesicle final transport, docking, and fusion with the plasma membrane.[2] Patch-clamp measurements and optical imaging indicate that vesicular release may involve either full collapse fusion (FCF) or "kiss and run" (K&R) processes.[1–3] Kiss and run could facilitate rapid cycling of vesicles, but its biological stipulation still remains highly debated.[1–3] During past two decades, electrochemical detection of release events from single mammalian cells[4] at microelectrodes has emerged to become one of the most powerful techniques for monitoring release of molecules in real-time and providing essential kinetic information on vesicular events.[4b,d,5] The recent development of novel electrochemical sensors with improved performance has greatly improved such microelectrode measurements.[6] Despite such successes, amperometric methods have been mostly applied to single animal cells. However, it has been suggested that plant hormones may be released by similar mechanisms.

Auxin, or indole acetic acid (IAA), is an essential, multifunctional plant hormone that influences virtually every aspect of plant growth and development.[7] Polar auxin transport is a unique feature of auxin action.[8] Recent biochemical results suggest that auxin efflux is mediated by a vesicular cycling mechanism,[7b,9] which indicates that in plant cells auxin would be carried by vesicles and released by polar exocytosis (Scheme 1 a).[1b,10] Though microscopic imaging could observe vesicles and vesicle fusion events,[11] and patch clamp techniques have been used to measure individual exocytotic events from plant cells,[12] there was still a lack of direct evidence in supporting this scenario by real-time monitoring of vesicle-carried auxin molecules release from single plant cells. So far, several groups reported the measurements of IAA using electrochemical methods.[13] However, insufficient sensitivity (usually with detection limits at μM or sub-μM level) of these sensors restricts their further application in the real-time monitoring of the very small number of IAA released from single plant cells.

Very recently, quasi-aligned nanofiber arrays (QANFAs) have been considered as one of the most promising architectures to enhance the electrochemical activity owing to a large surface-to-volume ratio, high catalytic abilities, and high electron transfer rate.[15] In our previous work, we developed a simple method to grow in situ core–shell titanium carbide–carbon QANFAs (TiC@C-QANFAs) on biomedical Ti6Al4V foils and wires.[14b,c] The nanofiber arrays displayed extremely fast electron-transfer kinetics and excellent electrochemical performance in the highly sensitive detection of biomolecules.[14b,c] Inspired by the excellent electrochemical performance of TiC@C-QANFAs and the scenario of quantal release of auxin, we demonstrated the construction of a novel micro-electrochemical sensor (TiC@C/Pt-QANFAs) for real-time monitoring of auxin efflux by exocytosis from single plant cells. This highly sensitive microsensor was obtained by loading uniformly dispersed platinum nanoparticles with high density and small sizes (3–6 nm) on TiC@C nanofiber arrays (Scheme 1), which showed extremely high sensitivity in the detection of IAA with a detection limit of 1.0 nM. Using this sensor, individual exocytotic vesicular release events of auxin

[*] J. T. Liu,[+] Y. L. Liu, Z. Cheng, S. J. Chen, Prof. W. H. Huang
Key Laboratory of Analytical Chemistry for Biology and Medicine (Ministry of Education), College of Chemistry and Molecular Sciences, Wuhan University, Wuhan 430072 (China)
E-mail: whhuang@whu.edu.cn
L. S. Hu,[+] Dr. R. S. Chen
School of Materials and Metallurgy
Wuhan University of Science and Technology, Wuhan 430081 (China)
Prof. C. Amatore
Ecole Normale Supérieure, Département de Chimie
UMR 8640 (CNRS-ENS-UPMC and LIA CNRS XiamENS)
24 rue Lhomond, 75005 Paris (France)
Prof. K. F. Huo
Wuhan National Laboratory for Optoelectronics
Huazhong University of Science and Technology
Wuhan 430074 (China)
E-mail: kfhuo@wust.edu.cn
[+] These authors contributed equally to this work.

[**] Supported by the National Natural Science Foundation of China (Nos. 91017013, 31070995, 21375099), the Program for Changjiang Scholars and Innovative Research Team in University (IRT1030), and UMR 8640 (CNRS-ENS-UPMC) and LIA CNRS XiamENS.
Supporting Information for this article is available on the WWW under http://dx.doi.org/10.1002/anie.201308972.

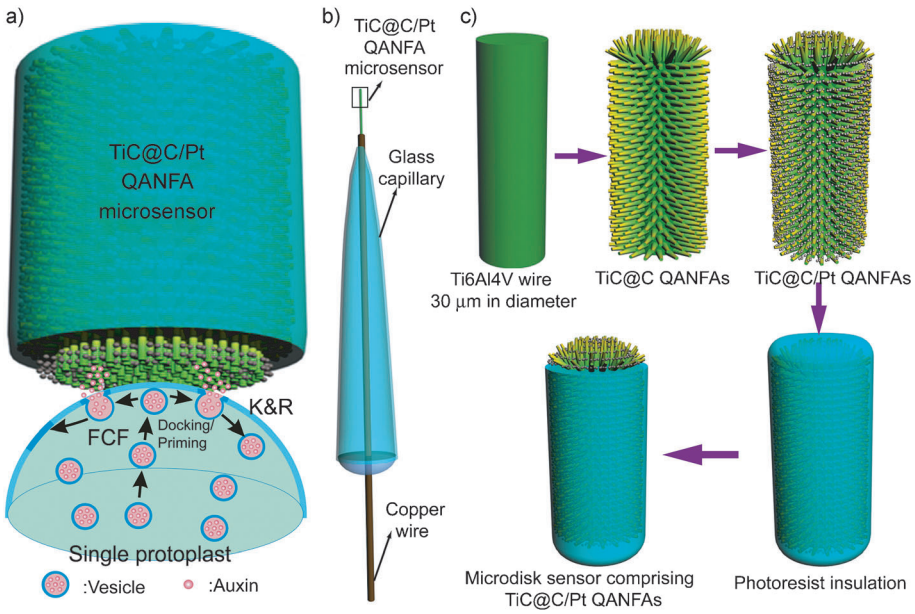

Scheme 1. a) Amperometric monitoring of auxin efflux from single protoplasts by vesicular exocytosis; b) the TiC@C/Pt-QANFAs microdisk sensor; c) the main processes for the fabrication of this sensor.

from single plant protoplasts were monitored in real time and quantified. Furthermore, this enabled a quantitative and kinetic characterization of single exocytotic events from plant protoplasts showing that they embrace two classes: simple full release events and complex "kiss and run" sequences.

To obtain a highly sensitive microsensor comprising TiC@C/Pt-QANFAs, we first used Ti6Al4V microwires (20–30 μm in diameter) as the starting materialand fabricated a microwire composed of TiC@C-QANFAs. To further improve the sensitivity for detection of smaller number of molecules, high-density single-crystalline platinum nanoparticles were synthesized on the TiC@C nanofibers by reduction of Pt precursor to form a micro-cylindrical TiC@C/Pt-QANFAs sensor (Scheme 1 a,b).

Figure 1 a, b shows representative low- and high-magnification field-emission scanning electron microscopy (FE-SEM) images of the sensor, which indicate that this procedure led to uniform nanofibers covering the surface (both top and side) of Ti alloy wire forming three-dimensional (3D) nanofiber arrays. The transmission electron microscopy (TEM) image (inset in Figure 1 b) shows that the nanofibers covered by a layer of uniform nanoparticles have diameters of between 90 and 110 nm. The X-ray diffraction (XRD) pattern (Figure 1 c) reveals main diffraction peaks at 39.8, 46.3, 67.9, 81.4, and 86.7° corresponding to the (111), (200), (220), (311), and (222) planes of face-centered cubic (fcc) structure of Pt (JCPDS card: 4-802) respectively. The element distribution is also analyzed by X-ray energy dispersive spectrometer (EDS; Supporting Information, Figure S1). The X-ray photoelectron spectroscopy (XPS) survey spectrum (Figure 1 d) establishes that the nanofiber arrays are composed of Pt, C, and O (the O peak originates from surface adsorption). TEM further shows a number of uniform nanoparticles tightly attached onto the surface of the TiC@C nanofibers, leading to the formation of the heterostructured nanofibers (Figure 1 e). The high resolution TEM (HR-TEM) image (Figure 1 f) reveals that these nanoparticles have sizes of 3–6 nm and an interplane distance of about 0.225 nm, corresponding to the (111) plane of metallic Pt, in full agreement with the XRD and XPS observations.

To improve the signal-to-noise ratio for single cell detection, the whole electroactive area of the cylindrical sensor was insulated with photoresist followed by immersion of the tip area into a developing solution described in our previous work[15] to expose the desired electroactive area (Scheme 1 b). The SEM results show that all the electroactive area is well-insulated (Figure 2 a) and TiC@C/Pt-QANFAs on the tip of the sensor is selectively exposed (Figure 2 b), forming a microdisk-shaped electrochemical sensor.

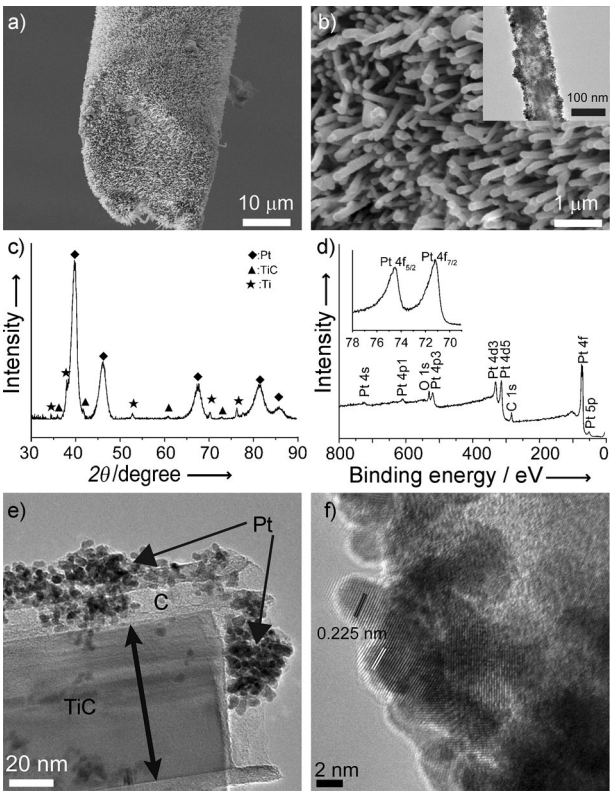

Figure 1. a) Low-magnification and b) high-magnification FE-SEM images of the TiC@C/Pt-QANFA microelectrode; c) XRD pattern and d) XPS survey scan of the 3D nanofiber arrays on Ti alloy wire; e) Enlarged TEM and f) HR-TEM image of a single TiC@C/Pt-QANFA. The inset in (b) and (d) are the TEM image of a nanofiber and high-resolution Pt4f spectrum, respectively.

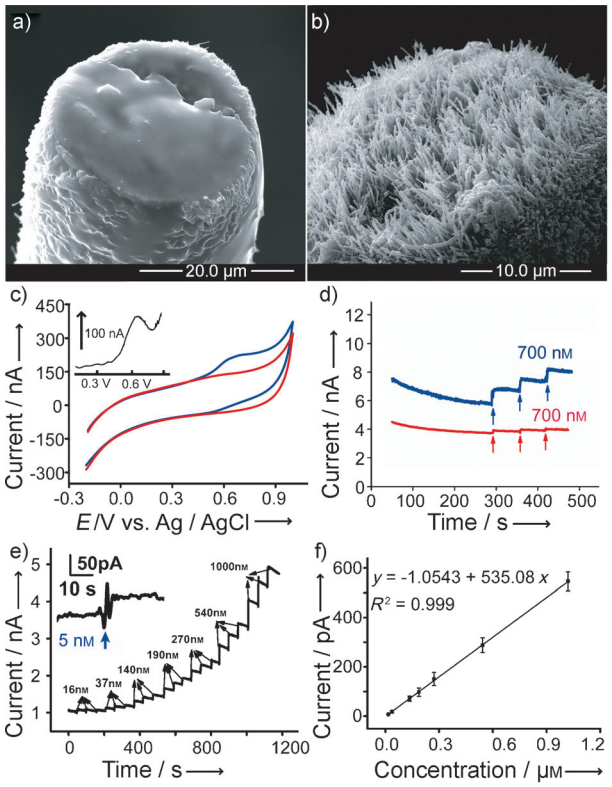

Figure 2. SEM images of a TiC@C/Pt-QANFA microelectrode insulated with AZ5214 (a) and after washing (b) with H_2SO_4/H_2O_2(v/v=7:3); c) Cyclic voltammograms obtained from the TiC@C/Pt-QANFA microelectrode in PBS in the absence of IAA (red line) and in the presence of 10^{-4} M IAA (black line) at a scanning rate of 100 mVs^{-1} (inset: differential pulse voltammograms (DPV) of IAA); d) amperometric response curves of a TiC@C/Pt-QANFA microelectrode (black line) and TiC@C microelectrode (red line) to a series of increases of IAA concentration in PBS solution; e) typical amperometric responses of the TiC@C/Pt-QANFA microelectrode to successive additions of IAA at applied potentials of 0.6 V (vs. Ag/AgCl) in PBS solution; f) calibration plot of amperometric currents against concentrations of IAA over the concentration range from 16 nM to 1.0 μM.

Figure 2c shows cyclic voltammograms of IAA 0.1 mM obtained with the TiC@C/Pt-QANFAs microdisk sensor. An irreversible oxidation peak with peak potential of 0.60 V is obtained (Figure 2c). Note that this value is much lower than previously reported (usually over the range of 0.70–0.90 V[13b–d,16]) and also lower than that on TiC@C-QANFAs (Supporting Information, Figure S2), indicating the excellent electrocatalytic properties toward oxidation of IAA. The calculated electron stoichiometry was two, affording a cation of 3-methyleneindolenine carboxylic acid, in agreement with previous reports.[13a–d] The amperometric response of 0.7 μM IAA at TiC@C/Pt-QANFAs microsensor is approximately 5-fold greater than that at TiC@C-QANFAs (Figure 2d). The excellent electrochemical behavior could be attributed to the synergistic effects of high electrocatalytic activities of high density Pt single crystalline nanoparticles[17] and fast electron-transfer rate of the unique core–shell structure.[14b] Figure 2e shows the amperometric responses of the TiC@C/Pt-QANFAs microsensor to successive additions of IAA. Furthermore, this sensor displays excellent linear amperometric response over the IAA concentration range of interest (Figure 2f), with a detection limit of 1.0 nM (S/N = 3), being at least 20 times better than those reported previously.[13a–d]

Unlike mammalian cells, which tightly adhere onto substrates, protoplasts or plant cells are not easily immobilized on the substrate. To immobilize single protoplasts, we developed a robust and versatile technique that use an agarose microwell array chip for large-scale single-cell trapping and immobilization (Supporting Information, Figure S3). The single protoplasts were well-dispersed into each microwell and tightly immobilized inside the microwells (Supporting Information, Figure S2h).

To monitor the vesicular exocytosis from single plant cells in real time, the electroactive area of the TiC@C/Pt-QANFAs microsensor was placed to touch the cell surface of single plant protoplasts isolated from young developing leaves of oilseed rape. The exocytosis was evoked by high K^+ (80 mM) solution to induce membrane depolarization and vesicle fusion with plasma membrane. Figure 3a presents typical results depicting amperometric monitoring of exocytotic events from a single protoplast. Release events were recorded as a number of clearly resolvable transient amperometric spikes from all of the protoplasts that were monitored. Detection of brief spikes with average short time-width $T_{1/2}$ (0.95 ± 0.04 ms, mean $\pm$s.e.m.) indicates extremely fast release kinetics from membrane-fused vesicles as well as rapid oxidation of the released auxin by the TiC@C/Pt-QANFA microsensor.

Previous electrophysiological results from capacitance measurements of membranes attached to cells revealed that, similar to animal cells, plant cells release secretory product by both FCF and K&R.[12,18] Interestingly, thanks to its high temporal resolution, our amperometric results clearly exhibit these two distinctive release modes. Most spikes (ca. 85%, 328 spikes were identified as simple events from 386 events from 7 protoplasts), denoted as "simple" events, display single rising and single falling phases (inset in Figure 3a), while the remaining ones (58 from 386 events), classified as "complex events", exhibited complex release kinetics consisting of multiple, well-defined much shorter rising and falling phases (Figure 3b).

Figure 3c displays statistical results for some parameters (peak amplitude I_{peak}, time width at half maximum $T_{1/2}$, charge Q) of the individual "quantal" release from the single protoplasts respectively. Q is a measure of the vesicular content and $T_{1/2}$ represents the kinetics of the vesicular exocytotic events, while I_{peak} integrates both aspects. Simple events yielded the mean values of $I_{peak} = 245 \pm 7$ pA and $Q = 299 \pm 16$ fC (mean $\pm$s.e.m., averaged 328 spikes). The average $T_{1/2}$ was 0.95 ± 0.04 ms, indicating the fast kinetics of the vesicular exocytotic events. Complex events showed significantly longer durations ($T_{1/2} = 1.94 \pm 0.17$ ms, here $T_{1/2}$ represents the duration of the whole complex events, $n = 58$ events; see Figure 3b right) and released overall a greater number of molecules ($Q = 459 \pm 56$ fC, $n = 58$ events) with much smaller average amplitude ($I_{peak} = 185 \pm 7$ pA, $n = 136$ spikes from 58 complex events).[19] The significantly different statistics between simple and complex events clearly indicate two distinct fusion modes of exocytotic mechanisms. The

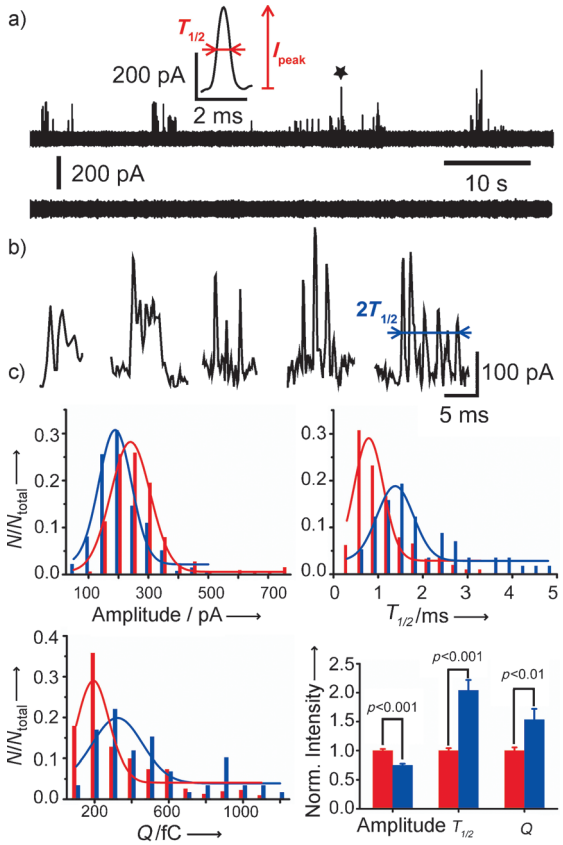

Figure 3. a) A typical amperometric trace showing multiple transient amperometric spikes detected (upper trace) as IAA is released from a single protoplast stimulated by high K^+ solution and no spike is found without high K^+ evoking (lower trace); b) representative examples of complex events; c) histograms of simple (red, $n=328$ simple events) versus complex event characteristics (blue, $n=136$ spikes from 58 complex events) in I_{peak}, $T_{1/2}$, and K obtained from amperometric recordings (from 7 protoplasts using one microelectrode). For the complex events, all the 136 spikes were counted for I_{peak}, while 58 events were considered for $T_{1/2}$ and Q; the solid lines represent the Gaussian functions fitted to the data, error bars represent standard errors, and an independent-samples T-test was used to calculate P values.

complex events could result from single vesicles forming rapidly flickering fusion pores, as was previously described in tobacco BY-2 protoplasts[12c] as well as in rat ventral midbrain neurons for mammals.[5]

To provide evidence that the amperometric spikes resulted from the oxidation of IAA molecules released from single protoplasts, several experiments have been performed to validate this matter. Firstly, ELISA results from bulk measurements on the population level showed that, compared to control assay, IAA content in supernatants of cell culture medium was increased by 2.2 fold when high K^+ solution was added into the medium to cause the plasma membrane depolarization (Supporting Information, Figure S4), indicating that high K^+ stimulation could effectively increase the extracellular IAA concentration by promoting IAA efflux.

Pre-loading plant cells with higher concentration of IAA to induce the influx of IAA and to increase the cytoplasmic IAA concentration is a common and effective approach to study the behaviors and mechanisms of auxin efflux.[20] Here, we increased the amount of readily releasable IAA molecules by pre-loading IAA for 30 min before amperometric detection. The detection results showed that amperometric traces with much larger peak amplitude and higher peak charge (Supporting Information, Figure S4) were obtained. The average I_{peak} and Q were 676 ± 22 pA and 2300 ± 121 fC (mean $\pm$ s.e.m.), corresponding to about 2.8-fold and 7.7-fold of that from single protoplasts without IAA preloading respectively (comparison is restricted to simple events only). The results demonstrated that the quantal size of IAA was significantly increased with the increasing of cytoplasmic IAA concentration by pre-loading, further validating IAA efflux from single protoplasts by vesicular exocytosis.

Furthermore, we used an inhibitor of auxin efflux- 1-*N*-naphthylphthalamic acid (NPA)[7b,21] to block auxin efflux. Our results presented a dramatic decrease in both detection probability and amperometric frequency, and only a few amperometric spikes (4–5 spikes) with very small I_{peak} values were recorded from 4% protoplasts, which suggested that IAA efflux was almost completely inhibited by NPA. These results further confirmed that the amperometric spikes detected in the electrochemical traces (Figure 3; Supporting Information, Figure S5) represent elementary vesicular quantal release of IAA triggered by K^+.

In summary, we developed a TiC@C/Pt-QANFAs microelectrochemical sensor for real-time monitoring of IAA efflux by exocytosis from single plant cells. This sensor showed extremely high sensitivity in detection of IAA with a DL of 1.0 nM. Using this sensor, the quantal release of auxin from single plant protoplast by exocytosis was monitored in real time and quantified. The exocytotic release of IAA was further validated by ELISA assay, IAA pre-loading and NPA inhibitor experiments. Our results provide direct evidence that IAA efflux involves a vesicular exocytosis mechanism with fast kinetics, displaying both FCF and K&R modes. Taken together, the capability of real-time monitoring of IAA efflux by vesicular exocytosis from single plant cells should open up opportunities for elucidating the mechanism of plant growth regulation by IAA polar transport and efflux.

Received: October 15, 2013
Published online: January 30, 2014

Keywords: amperometric monitoring · auxin efflux · electrochemical sensors · exocytosis · single plant cells

[1] a) R. D. Burgoyne, A. Morgan, *Physiol. Rev.* **2003**, *83*, 581–632; b) T. C. Südhof, J. Rizo, *Cold Spring Harbor Perspect. Biol.* **2011**, *3*, a005637. Note that the Nobel Prize in Physiology or Medicine 2013 was recently awarded to J. E. Rothman, R. W. Schekman, and T. C. Südhof for their discovery of the machineries regulating vesicle traffic in cells.
[2] a) E. D. Gundelfinger, M. M. Kessels, B. Qualmann, *Nat. Rev. Mol. Cell Biol.* **2003**, *4*, 127–139; b) V. Haucke, E. Neher, S. J. Sigrist, *Nat. Rev. Neurosci.* **2011**, *12*, 127–138.
[3] L. He, L. G. Wu, *Trends Neurosci.* **2007**, *30*, 447–455.
[4] a) R. M. Wightman, J. A. Jankowski, R. T. Kennedy, K. T. Kawagoe, T. J. Schroeder, D. J. Leszczyszyn, J. A. Near, E. J. Diliberto, Jr., O. H. Viveros, *Proc. Natl. Acad. Sci. USA* **1991**, *88*,

10754 – 10758; b) E. V. Mosharov, D. Sulzer, *Nat. Methods* **2005**, *2*, 651 – 658; c) A. Schulte, W. Schuhmann, *Angew. Chem.* **2007**, *119*, 8914 – 8933; *Angew. Chem. Int. Ed.* **2007**, *46*, 8760 – 8777; d) C. Amatore, S. Arbault, M. Guille, F. Lemaitre, *Chem. Rev.* **2008**, *108*, 2585 – 2621; e) Y. X. Huang, D. Cai, P. Chen, *Anal. Chem.* **2011**, *83*, 4393 – 4406; f) R. Trouillon, M. K. Passarelli, J. Wang, M. E. Kurczy, A. G. Ewing, *Anal. Chem.* **2013**, *85*, 522 – 542.

[5] a) R. G. W. Staal, E. V. Mosharov, D. Sulzer, *Nat. Neurosci.* **2004**, *7*, 341 – 346; b) R. M. Wightman, C. L. Haynes, *Nat. Neurosci.* **2004**, *7*, 321 – 322.

[6] a) H. G. Sudibya, J. M. Ma, X. C. Dong, S. Ng, L. J. Li, X. W. Liu, P. Chen, *Angew. Chem.* **2009**, *121*, 2761 – 2764; *Angew. Chem. Int. Ed.* **2009**, *48*, 2723 – 2726; b) K. L. Adams, B. K. Jena, S. J. Percival, B. Zhang, *Anal. Chem.* **2011**, *83*, 920 – 927; c) A. Meunier, O. Jouannot, R. Fulcrand, I. Fanget, M. Bretou, E. Karatekin, S. Arbault, M. Guille, F. Darchen, F. Lemaître, C. Amatore, *Angew. Chem.* **2011**, *123*, 5187 – 5190; *Angew. Chem. Int. Ed.* **2011**, *50*, 5081 – 5084; d) C. X. Guo, S. R. Ng, S. Y. Khoo, X. T. Zheng, P. Chen, C. M. Li, *Acs Nano* **2012**, *6*, 6944 – 6951; e) X. L. Lu, H. J. Cheng, P. C. Huang, L. F. Yang, P. Yu, L. Q. Mao, *Anal. Chem.* **2013**, *85*, 4007 – 4013.

[7] a) A. W. Woodward, B. Bartel, *Ann. Bot.* **2005**, *95*, 707 – 735; b) S. Vanneste, J. Friml, *Cell* **2009**, *136*, 1005 – 1016.

[8] a) W. D. Teale, I. A. Paponov, K. Palme, *Nat. Rev. Mol. Cell Biol.* **2006**, *7*, 847 – 859; b) F. Santos, W. Teale, C. Fleck, M. Volpers, B. Ruperti, K. Palme, *Plant Biol.* **2010**, *12*, 3 – 14; c) J. Dettmer, J. Friml, *Curr. Opin. Cell Biol.* **2011**, *23*, 686 – 696.

[9] E. Zažimalová, P. Křeček, P. Skupa, K. Hoyerová, J. Petrášek, *Cell. Mol. Life Sci.* **2007**, *64*, 1621 – 1637.

[10] a) N. Geldner, J. Friml, Y. D. Stierhof, G. Jurgens, K. Palme, *Nature* **2001**, *413*, 425 – 428; b) J. Friml, K. Palme, *Plant Mol. Biol.* **2002**, *49*, 273 – 284; c) G. K. Muday, W. A. Peer, A. S. Murphy, *Trends Plant Sci.* **2003**, *8*, 301 – 304; d) G. Li, H. W. Xue, *Plant Cell* **2007**, *19*, 281 – 295.

[11] a) X. H. Wang, Y. Teng, Q. L. Wang, X. J. Li, X. Y. Sheng, M. Z. Zheng, J. Samaj, F. Baluska, J. X. Lin, *Plant Physiol.* **2006**, *141*, 1591 – 1603; b) K. Toyooka, Y. Goto, S. Asatsuma, M. Koizumi, T. Mitsui, K. Matsuoka, *Plant Cell* **2009**, *21*, 1212 – 1229.

[12] a) G. Thiel, N. Battey, *Plant Mol. Biol.* **1998**, *38*, 111 – 125; b) R. Weise, M. Kreft, R. Zorec, U. Homann, G. Thiel, *J. Membr. Biol.* **2000**, *174*, 15 – 20; c) V. Bandmann, M. Kreft, U. Homann, *Mol.Plant* **2011**, *4*, 241 – 251.

[13] a) T. Hu, G. Dryhurst, *J. Electroanal. Chem.* **1993**, *362*, 237 – 248; b) K. Wu, Y. Sun, S. Hu, *Sens. Actuators B* **2003**, *96*, 658 – 662; c) Y. Yardım, M. E. Erez, *Electroanalysis* **2011**, *23*, 667 – 673; d) J. Bulíčková, R. Sokolová, S. Giannarelli, B. Muscatello, *Electroanalysis* **2013**, *25*, 303 – 307; e) E. S. McLamore, A. Diggs, P. C. Marzal, J. Shi, J. J. Blakeslee, W. A. Peer, A. S. Murphy, D. M. Porterfield, *Plant J.* **2010**, *63*, 1004 – 1016.

[14] a) L. S. Hu, K. F. Huo, R. S. Chen, X. M. Zhang, J. J. Fu, P. K. Chu, *Chem. Commun.* **2010**, *46*, 6828 – 6830; b) R. S. Chen, L. S. Hu, K. F. Huo, J. J. Fu, H. W. Ni, Y. Tang, P. K. Chu, *Chem. Eur. J.* **2011**, *17*, 14552 – 14558; c) L. M. Li, X. Y. Wang, L. S. Hu, R. S. Chen, Y. Huang, S. J. Chen, W. H. Huang, K. F. Huo, P. K. Chu, *Lab Chip* **2012**, *12*, 4249 – 4256.

[15] F. Y. Du, W. H. Huang, Y. X. Shi, Z. L. Wang, J. K. Cheng, *Biosens. Bioelectron.* **2008**, *24*, 415 – 421.

[16] R. A. de Toledo, C. M. P. Vaz, *Microchem. J.* **2007**, *86*, 161 – 165.

[17] a) C. Wang, H. Daimon, T. Onodera, T. Koda, S. H. Sun, *Angew. Chem.* **2008**, *120*, 3644 – 3647; *Angew. Chem. Int. Ed.* **2008**, *47*, 3588 – 3591; b) Z. Y. Zhou, Z. Z. Huang, D. J. Chen, Q. Wang, N. Tian, S. G. Sun, *Angew. Chem.* **2010**, *122*, 421 – 424; *Angew. Chem. Int. Ed.* **2010**, *49*, 411 – 414.

[18] N. H. Battey, N. C. James, A. J. Greenland, C. Brownlee, *Plant Cell* **1999**, *11*, 643 – 659.

[19] Using Faraday's law, the charge Q corresponding to each spike is related to the number N of released molecules by $Q = nFN$, where n is the stoichiometric number of electrons of the Faradic detection (two for auxin oxidation) and F is the Faraday constant (96500); the fact that average Q from complex events is larger than that from single events is possibly due to the fact that complex events involve "kiss and run" from few linked vesicles, such as clustered vesicles or vesicles fused with each other before release, or from the fact that such events happen mostly during release by very large vesicles as a consequence of their size. For variations of release mode with vesicle sizes, see for example: L. A. Sombers, H. J. Hanchar, T. L. Colliver, N. Wittenberg, A. Cans, S. Arbault, C. Amatore, A. G. Ewing, *J. Neurosci.* **2004**, *24*, 303 – 309.

[20] a) B. Noh, A. S. Murphy, E. P. Spalding, *Plant Cell* **2001**, *13*, 2441 – 2454; b) E. Remy, T. R. Cabrito, P. Baster, R. A. Batista, M. C. Teixeira, J. Friml, I. Sa-Correia, P. Duque, *Plant Cell* **2013**, *25*, 901 – 926.

[21] J. Petrasek, J. Friml, *Development* **2009**, *136*, 2675 – 2688.

